GA–A22361

ENHANCED PERFORMANCE DISCHARGES IN THE DIII–D TOKAMAK WITH LITHIUM WALL CONDITIONING

by
G.L. JACKSON, E.A. LAZARUS, G.A. NAVRATIL, R. BASTASZ, N.H. BROOKS, D.T. GARNIER, K.L. HOLTROP, J.C. PHILLIPS, E.S. MARMAR, T.S. TAYLOR, D.M. THOMAS, W.R. WAMPLER, D.G. WHYTE, and W.P. WEST

OCTOBER 1996

GA–A22361

ENHANCED PERFORMANCE DISCHARGES IN THE DIII–D TOKAMAK WITH LITHIUM WALL CONDITIONING

by
G.L. JACKSON, E.A. LAZARUS,[†] G.A. NAVRATIL,[‡] R. BASTASZ,[◊]
N.H. BROOKS, D.T. GARNIER,[∆] K.L. HOLTROP, J.C. PHILLIPS,
E.S. MARMAR,[∆] T.S. TAYLOR, D.M. THOMAS, W.R. WAMPLER,[#]
D.G. WHYTE,[£] and W.P. WEST

This is a preprint of a paper to be presented at the 12th International Conference on Plasma Surface Interactions on Controlled Fusion Devices, May 20–24, 1996, Saint-Raphael, France and to be published in the *Proceedings*.

[†]Oak Ridge National Laboratory
[‡]Columbia University
[◊]Sandia National Laboratories, Livermore
[∆]Massachusetts Institute of Technology
[#]Sandia National Laboratories, Albuquerque
[£]INRS—Energie et Materiaux

Work supported by
the U.S. Department of Energy
under Contract Nos. DE-AC03-89ER51114, W-7405-ENG-48,
and DE-AC05-96OR22464

GA PROJECT 3466
OCTOBER 1996

ABSTRACT

Lithium wall conditioning has been used in a recent campaign evaluating high performance negative central shear (NCS) discharges. During this campaign, the highest values of stored energy (4.4 MJ), neutron rate (2.4×10^{16}/s), and $nT_i\tau$ (7×10^{20} m^{-3}-keV-s) achieved to date in DIII–D were obtained. High performance NCS discharges were achieved prior to beginning lithium conditioning, but it is clear that shot reproducibility and performance were improved by lithium conditioning. Central and edge oxygen concentrations were reduced after lithium conditioning. Lithium conditioning, consisting of up to four pellets injected at the end of the preceding discharge, allowed the duration of the usual inter-shot helium glow discharge to be reduced and reproducible high auxiliary power discharges, $P_{NBI} \leq$ 22 MW, were obtained with plasma currents up to 2.4 MA.

1. INTRODUCTION

A lithium pellet injector has been installed on DIII–D to apply a coating of lithium to the surface of the DIII–D graphite tiles. The goal of this wall conditioning is to reduce recycling and light atom impurity influxes for high triangularity discharges where the present DIII–D active cryopump is not effective because of geometrical constraints. Lithium pellets were first injected into eight VH–mode reference discharges to commission the injector. During these discharges, pellets injected into the current rampup phase triggered brief (< 200 ms) phases of enhanced confinement with characteristics similar to the lithium pellet enhanced performance (PEP) mode reported on the C-Mod device [1]. Lithium pellet injection was then used during a campaign to evaluate negative central shear (NCS) discharges. In this paper we describe the effect of lithium conditioning on these high performance discharges.

Lithium pellet injection was first used on Alcator C as a diagnostic to measure the current density profile [2]. In similar work on the TFTR tokamak it was observed that lithium pellets also affected recycling and impurity influx [3] leading to the use of lithium pellet injection on TFTR as a routine wall conditioning technique results in dramatically improved confinement for supershot discharges [4]. Despite the success of lithium conditioning on TFTR, other devices, e.g. JIPP-TIIU, TdeV, and C-Mod, have reported modest or no improvement after the application of lithium [5,6,7].

The DIII–D lithium pellet injector follows closely the design of the MIT Alcator C-Mod injector [8], and was constructed in collaboration with the MIT Plasma Fusion Center group. It is a four barrel injector (four pellets per discharge) and can be upgraded to increase the number of injected pellets if necessary. Two sizes of pellets are available: 1.5 mm^3 and 4.5 mm^3 producing an equivalent change in electron density of 1.0 and $2.9 \times 10^{19}/m^3$ respectively. Pellet velocity can be varied, but typical speeds are 500–600 m/s using helium propellant. Pellets are injected 15 cm above the midplane. Equivalent lithium deposition for the large pellet is 2/3 monolayer assuming uniform distribution over the DIII-D centerpost or ten monolayers if the lithium were deposited in a 10 cm annulus on the floor. Actual deposition will be discussed in Section 3.

In this paper we refer to high performance DIII–D discharges which we define as: I_p > 1.6 MA, W_{MHD} > 2 MJ, P_{NB} > 10 MW, and $\tau_{th}/\tau_{JET\text{-}DIII\text{–}D} > 1$.

2. LITHIUM CONDITIONING IN DIII–D

The effect of lithium pellet injection on both central oxygen and central carbon concentrations is plotted in Fig. 1. Central concentrations were determined by: UV impurity charge exchange lines, calculated neutral beam penetration which is benchmarked against emission from the motional Stark effect diagnostic, and electron density profiles measured by Thomson Scattering. Concentrations in Fig. 1 were averaged from 500 to 1000 ms for discharges with 10 MW ≤ $P_{nb\ max}$ ≤ 22 MW over 6 days of the December 1995 high performance NCS campaign [9]. Up to four lithium pellets were injected into the end of several discharges with most of the lithium on the last day. Cumulative lithium injection during this campaign is shown also shown in Fig. 1. Pellets before discharge #87934 were used primarily for system checkout. A controlled experiment using lithium conditioning was not possible during this period and discharge conditions, e.g. shape and beam power varied throughout this sequence, although the strike point locations remained approximately fixed. There is a noticeable decline in central oxygen concentration when lithium conditioning is applied, particularly when comparing high plasma current discharges, shown as solid squares. There is little or no reduction in central carbon concentration with lithium conditioning, although carbon is the dominant central impurity. During this campaign, similar high performance discharges were periodically used to evaluate machine conditions. Three discharges, shown by arrows in Fig. 1 are compared in Fig. 2. After lithium conditioning (one pellet was injected at the end of discharge #87935 and three pellets for #87967), there is a reduction in both central oxygen and edge oxygen inferred from impurity line radiation, although again, no consistent reduction in carbon was noted. Although all discharges had the same neutral beam power (3.6 MW) from 300 to 2000 ms, differences in programming the neutral beam rampup phase from 2000 to 2250 ms caused differences in the time of peak stored energy.

Although the three 2.0 MA discharges plotted in Fig. 2 allow a comparison of the effect of lithium conditioning, there was little change in the global plasma parameters such as peak stored energy or neutron rate. Lithium conditioning can play a more important role in higher current discharges. A comparison of three such discharges, I_p =2.4 MA, $P_{nb\ max}$ =12.7–15.9 MW, is shown in Fig. 3. Two of these discharges were during a period characterized by locked modes and disruptions. Although the discharge evolution up to 2.2 s. differed in these cases, all oxygen lines and central oxygen concentration were lower after lithium conditioning (#87979). Central carbon concentrations were actually higher but the incremental increase during the high performance phase was less for the discharge with lithium conditioning. MHD activity [Fig. 3(c)] was lower for the lithium conditioned discharge and the onset of these MHD oscillations were delayed.

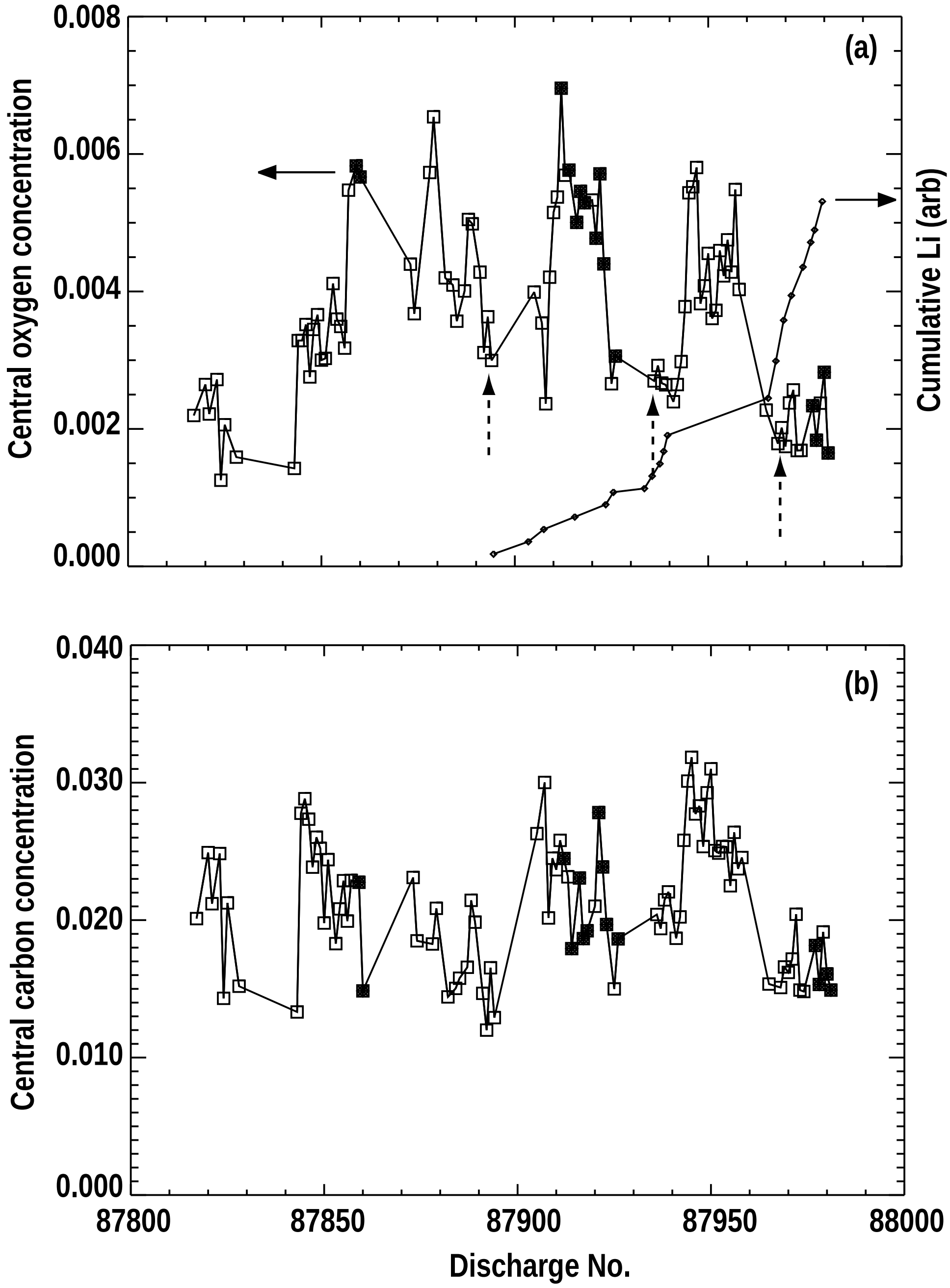

Fig. 1. Central oxygen concentration, (a), and central carbon concentration (b) for most beam heated discharges over a six day negative central shear campaign. Solid squares are for highest current discharges, >2.2 MA. Cumulative lithium injected during this campaign is also plotted. Highest performance discharges, producing record values of R_{DD}, W_{MHD}, and $nT_i\tau$ occurred at the end of this campaign with lithium conditioning.

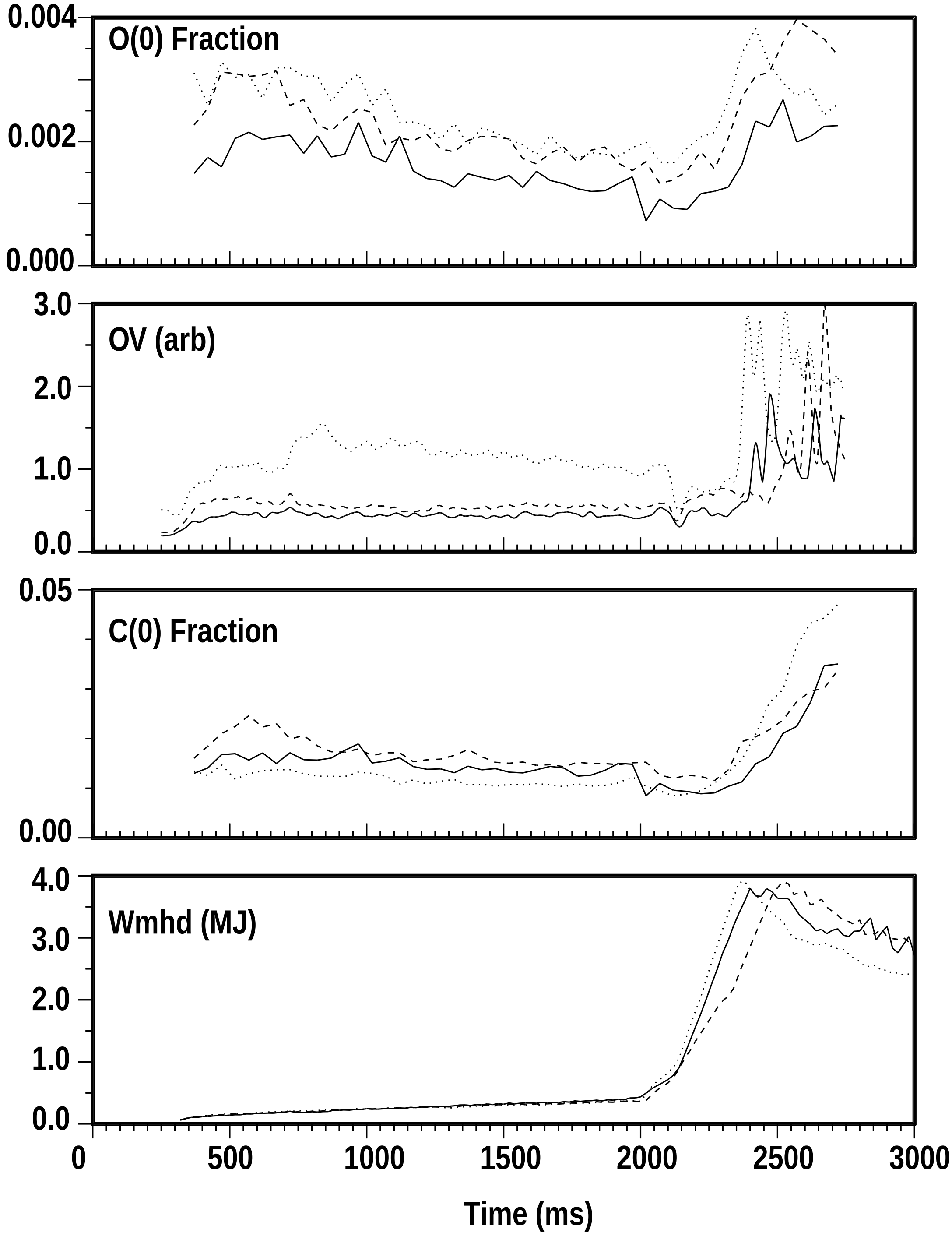

Fig. 2. Time evolution of oxygen and carbon impurities for three similar discharges shown by arrows in Fig. 1; I_p = 2 MA, B_T = 2.1 T, P_{NB} (0.3–2.0 s) = 3.6 MW, and P_{NB} (2.15–2.75 s) = 18.5–20.9 MW.

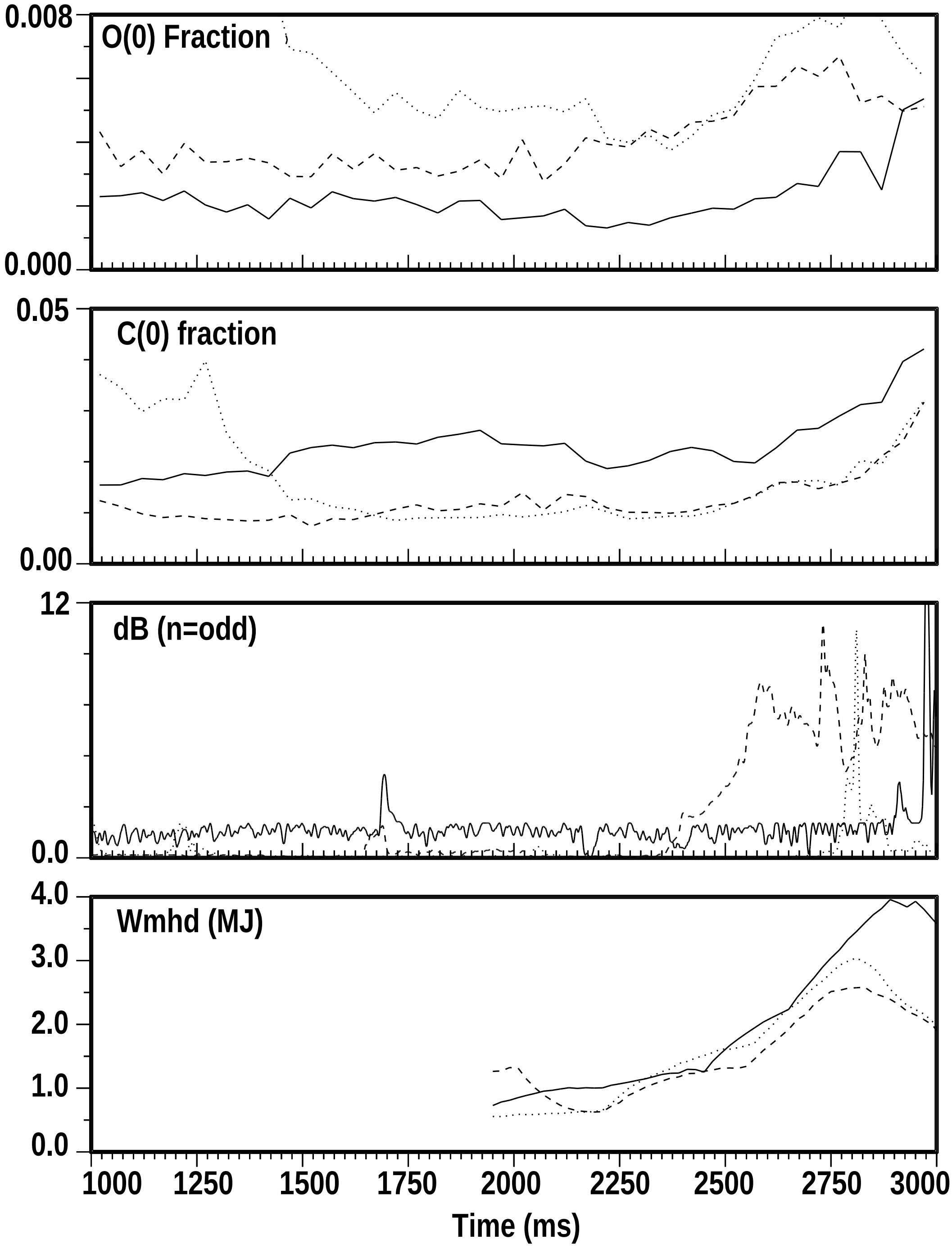

Fig. 3. Central oxygen (a) and carbon (b) concentrations for highest current (2.4 MA) discharges during the NCS campaign. Discharge #87979 (solid lines) was during the period of maximum lithium conditioning. Other discharges, with no lithium conditioning were during a shot sequence dominated by locked modes, e.g. #87923 (dotted lines) and disruptions. Although discharge #87925 (dashed lines) had no locked modes, MHD oscillations (c) were higher than other discharges. Highest stored energy (d) was achieved after lithium conditioning.

During the last sequence of high current discharges, I_p >2.2 MA, shown in Fig. 1 no disruptions or locked mode activity was observed, as opposed to earlier in the campaign when nearly all high current discharges before #87930 exhibited locked modes or disruptions. The high current discharges after #87975 produced the highest values of stored energy (4.4 MJ), neutron rate (2.4×10^{16}/s), and $nT_i\tau$ (7×10^{20} m^{-3}-keV-s) achieved to date in DIII–D. This last sequence was also accompanied by the most lithium conditioning during the campaign. However we note that several factors besides lithium conditioning may have contributed to the absence of disruptions and locked modes. In particular, the L to H transition time and early density evolution were varied between these sequences.

Helium glow conditioning before tokamak discharges is an important technique in DIII–D to obtain low recycling and high current reproducible discharges [10]. For best performance in reference VH–mode discharges, extending the glow duration from the standard five minute session to ten minutes is necessary [11]. The extensive use of lithium conditioning (e.g. shots 87966-87980) allowed a reduction in the glow time from ten minutes to eight minutes with no adverse affect on the next tokamak discharge. Since an eight minute glow did not adversely affect the time between tokamak discharges (limited by computer acquisition and power supply cool down), no glow scan was performed to further minimize the glow time.

3. DEPOSITION OF LITHIUM IN DIII–D

In order to evaluate the effectiveness of lithium pellet conditioning, it is important to assess lithium deposition. For the high triangularity discharges reported in this paper the strike points were approximately fixed, although the shape was varied during the discharge so that the dominant strike point was at the ceiling (in order to stay in L–mode), the floor (to induce H–mode) or approximately balanced. Lithium pellets were injected after the high performance phase, near the end of the discharge. Early injection during current ramp-up was not attempted in order not to affect the evolving negative central shear current density profile. The majority of lithium was injected into either a balanced double null configuration, or a shape with the lower null defining the last closed flux surface.

Lithium line radiation was observed by a midplane SPRED UV spectrometer and a visible divertor spectrometer. Except for anomalous events (e.g. locked modes, disruptions, or high MHD activity), lithium (LiIII) was only observed at the midplane during or immediately after pellet injection. Lithium (LiI and LiII) line radiation was observed by the divertor spectrometer after pellet injection and during the current ramp-up phase of the next tokamak discharge. However, as shown in Fig. 4, divertor lithium lines were only significantly above background for one discharge after pellet injection.

Lithium deposition was also monitored by long term floor coupons. After termination of the December 1995 NCS campaign, DIII–D was baked to 350°C, vented, and the coupons were removed. Lithium had only been deposited in a fixed configuration, i.e. the strike points did not vary. The deposition of this lithium on six coupons is shown in Fig. 5. We note that deposition occurred over the entire portion of the floor covered by the coupons, including directly under the high heat flux portion at the lower outer strike point. Furthermore, except for the outermost coupon, deposition appears quite uniform. Nuclear Reaction Analysis (NRA) detected 20% of the lithium 5 μm or more beneath the graphite coupon's surface.

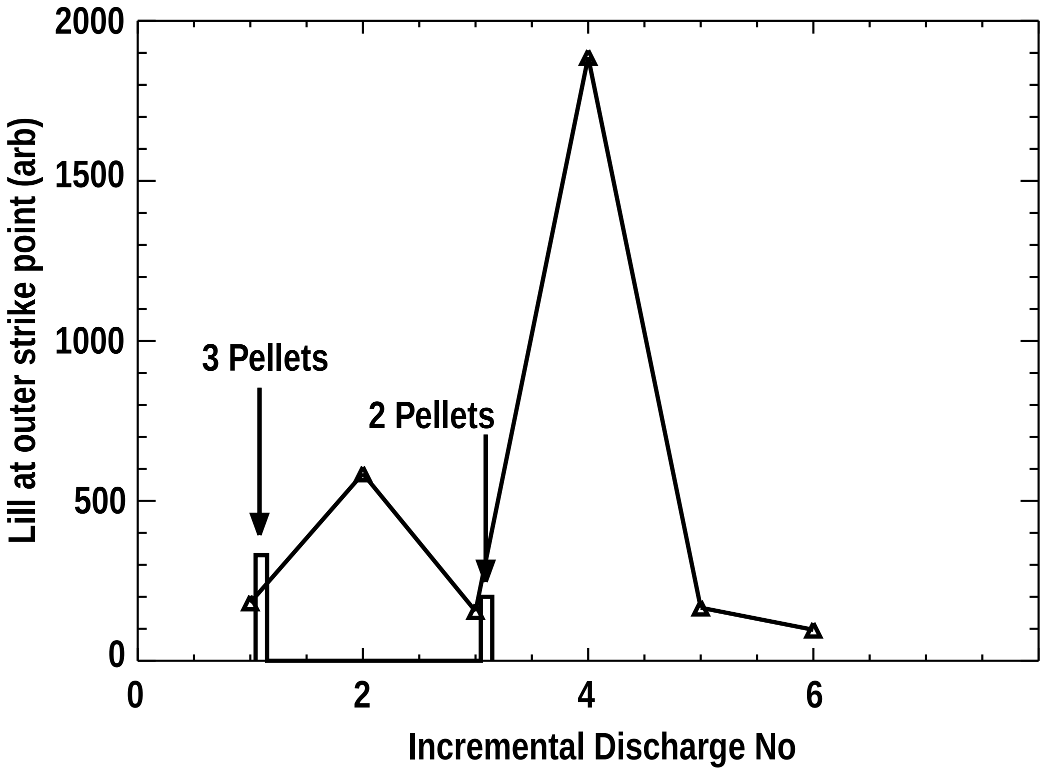

Fig. 4. Lithium visible line radiation (LiII) viewed at the outer lower divertor strike point, averaged during the current rampup phase. The number of pellets injected near the end of the discharge is also plotted. Early neutral beam power was higher for incremental shot #4, P_{NBI} (0.3–2.0 s) = 4.9 MW, than for the other discharges, P_{NBI} (0.3–2.0 s) = 3.6 MW.

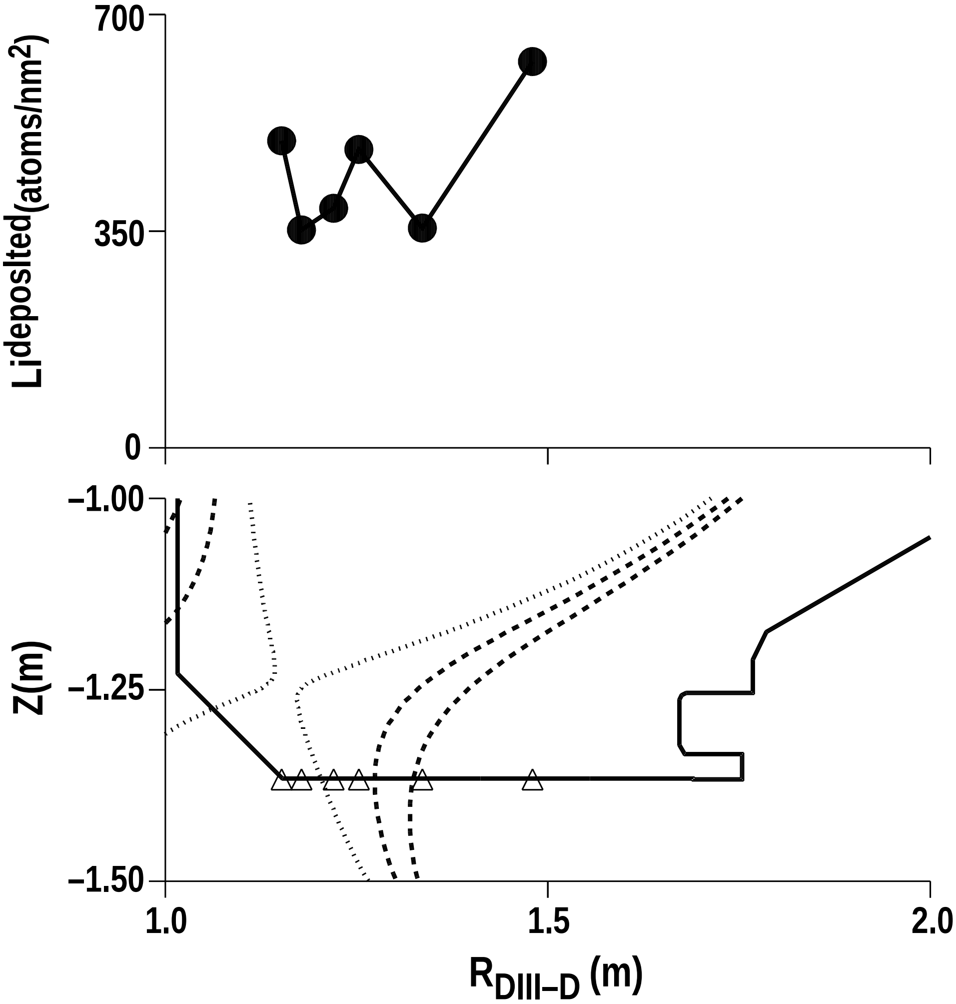

Fig. 5. Areal concentration of lithium, (a), measured by nuclear reaction analysis for six coupons removed after the NCS campaign. Position of the coupons are shown as triangles, (b), relative to the lower outer strike point and scrape off region (5 mm and 10 mm SOL are shown as dashed lines). Outline of the DIII–D plasma facing graphite surface is also shown.

4. DISCUSSION

The use of lithium pellet conditioning in DIII–D has had the most notable effect in the reduction of oxygen, both central and edge, even though oxygen is not the dominant impurity. Other tokamaks have documented the importance of oxygen reduction [12], although the mechanism is not well understood. As shown in Figs. 1–3, the central oxygen concentrations in DIII–D are significantly less than those of carbon; quantitative measurements of edge oxygen and carbon were not done for these discharges. TFTR has reported the most substantial reduction in carbon, not oxygen [13].

Lithium conditioning was used for the highest performance DIII–D discharges. We note however that the correlation between this conditioning and high performance is somewhat circumstantial, since no dedicated experiment was performed to evaluate the effect of the lithium. The effect of the lithium conditioning is most noticeable for the highest current, highest performance discharges. Clearly oxygen was reduced after introduction of lithium. Furthermore, the last sequence of high current discharges did not disrupt or have locked modes and the time for inter-shot helium glow was reduced, which was not done during previous campaigns to achieve high performance discharges. However discharges with performance nearly as high as those with lithium conditioning were produced earlier in this campaign.

Although not shown here, reference VH–mode discharges at lower current, stored energy and neutron fluxes did not see appreciable changes in oxygen concentration after lithium conditioning. This may explain why other devices without as much auxiliary heating power and generally lower heat fluxes to the wall have observed little or no benefit from lithium conditioning [5,6,7].

Based on the floor coupons, lithium appears to be deposited in a broad region of the scrape off layer. Lithium also is observed to a surprising depth, even in regions exposed to high heat flux. Calculations of nuclear stopping distance indicate that lithium should not penetrate further than 100 Å [14], although lithium was measured to depths of 2×10^5 Å (20 μm). In this experiment, we cannot rule out baking as a possible mechanism to distribute and deposit the lithium, since DIII–D was subjected to a high temperature bake before the coupons were removed.

We can also estimate the uniformity of deposition by comparing the total amount of lithium injected to the areal density measured by the coupons. We estimate that 2.4×10^{22} Li atoms have been deposited in DIII–D by the pellet injector and the average areal density measured by the coupons is 450 Li atoms/nm^2. If Li concentrations are homogenous on the 70 m^2 of graphite surface, then the NRA analysis estimates a total of 3.2×10^{22} lithium atoms in DIII–D. These numbers are within the uncertainties in the measurements, and thus we conclude that lithium has been more or less uniformly deposited within DIII–D.

The time scale for the lithium to become uniformly deposited can only be roughly estimated. Data from Fig. 1, where lithium was not injected on every consecutive discharge, implies that the reduction in oxygen extends over several discharges. However, as shown in Fig. 4, lithium deposited in the divertor region is rapidly eroded on the time scale of a single shot. Since lithium is eventually deeply deposited in the graphite, its effect in reducing oxygen may be limited by lithium diffusion into the graphite. The transitory effect of lithium conditioning has also been observed on TFTR, where highest performance supershots require up to two preparatory discharges for lithium pellet injection [13] and lithium pellet injection is routinely used.

Although lithium pellet injection produced lower recycling in TFTR, no such reduction has been observed in DIII–D. There are several possible reasons for this. First peak heat flux to the graphite tiles is considerably lower in DIII–D diverted discharges than in TFTR inner wall limited discharges, so thermal desorption due to tile surface heating is less in DIII–D. Furthermore, helium glow conditioning is done before every DIII–D tokamak discharge to maintain recycling at a low level [10] and thus reductions in recycling with lithium conditioning might not be as pronounced in DIII–D. Finally, DIII–D lithium conditioning has been primarily done at the end of discharges, where the effect on recycling is expected to be less than if pellets are injected during the current ramp-up phase as done in TFTR. Furthermore, the quantity of lithium injected per discharge in DIII-D is significantly less; there has been no attempt yet to optimize DIII–D lithium conditioning.

In conclusion, lithium conditioning has been implemented in DIII–D and was used during a campaign to evaluate high performance NCS discharges. Lithium conditioning seems to be most effective in reducing oxygen and in locked mode avoidance for high current (>2.2 MA) discharges. The lithium appears to be uniformly distributed, although the time scale (i.e. the number of discharges) to accomplish this is still not determined. However, lithium is rapidly eroded (on the time scale of one discharge) in the divertor region. Future work will focus on optimizing lithium deposition, finding the operating space over which lithium conditioning is effective, and using lithium pellets during the current rampup phase to reduce recycling.

REFERENCES

[1] D.T. Garnier, E.S. Marmar, Y. Takase, *et al.*, Bull Am Phys. Soc. **40** (1995) 1780.

[2] E.S. Marmar, Bull Am Phys. Soc. **32** (1987)1847.

[3] J.L. Terry, E.S. Marmar, R.B. Howell, *et al.*, Proc. 11th Int. Conf. on Plasma Physics and Contr. Nuc. Fus. Res., (Washington, USA, 1990) IAEA, Vienna, 1991 CN-53/A-V-5.

[4] J.D. Strachan, D.K. Mansfield, M.G. Bell, J. Nucl. Mater. **217** (1994) 145.

[5] H. Sugai, H. Toyoda, K. Nakamura, *et al.*, J. Nucl. Mater. **220-222** (1995) 254.

[6] B. Terreault, H.Y. Guo, D. Keroack, *et al.*, J. Nucl. Mater. **220-222** (1995) 1130.

[7] J.A. Snipes, MIT Plasma Fusion Center, private communication (1995).

[8] D.T. Garnier, E.S. Marmar, C. Christensen, *et al.*, Bull Am Phys. Soc. **39** (1994) 1669.

[9] E.A. Lazarus, G. Navratil, C.M. Greenfield, *et al.*, submitted to Nuc. Fus. (1996).

[10] G.L. Jackson, T.S. Taylor, P.L. Taylor, Nucl. Fus. **30** (1990) 2305.

[11] K.L. Holtrop, G.L. Jackson, A.G. Kellman, to be presented at the 43rd symposium of the American Vacuum Society (1996).

[12] J. Winter, Plas. Phys. and Control. Fus., accepted for publication (1996).

[13] D.K. Mansfield, J.D. Strachan, M.G. Bell, *et al.*, Phys. Plasmas, **12** (1995) 4252.

[14] W.R. Wampler, Sandia National Laboratory, Albuquerque, private communication (1996).

ACKNOWLEDGMENTS

We gratefully acknowledge the support and assistance of the MIT Plasma Fusion Center group in the design and construction of the DIII–D lithium pellet injector. Work supported by U.S. Department of Energy under Contract Nos. DE-AC03-89ER51114, DE-AC05-OR9622464, and DE-AC04-94AL85000.